

Electron-Transfer Chemistry of Ru–Linker–(Heme)-Modified Myoglobin: Rapid Intraprotein Reduction of a Photogenerated Porphyrin Cation Radical

Chad E. Immoos,[†] Angel J. Di Bilio,[†] Michael S. Cohen,[†] Wytze Van der Veer,[†] Harry B. Gray,^{*,†} and Patrick J. Farmer^{*,†}

Department of Chemistry, University of California, Irvine, California 92697-2025, and Beckman Institute, California Institute of Technology, Pasadena, California 91125

Received February 28, 2004

We report the synthesis and characterization of RuC7, a complex in which a heme is covalently attached to a [Ru(bpy)₃]²⁺ complex through a –(CH₂)₇– linker. Insertion of RuC7 into horse heart apomyoglobin gives RuC7Mb, a Ru(heme)–protein conjugate in which [Ru(bpy)₃]²⁺ emission is highly quenched. The rate of photoinduced electron transfer (ET) from the resting (Ru²⁺/Fe³⁺) to the transient (Ru³⁺/Fe²⁺) state of RuC7Mb is >10⁸ s⁻¹; the back ET rate (to regenerate Ru²⁺/Fe³⁺) is 1.4 × 10⁷ s⁻¹. Irreversible oxidative quenching by [Co(NH₃)₅Cl]²⁺ generates Ru³⁺/Fe³⁺: the Ru³⁺ complex then oxidizes the porphyrin to a cation radical (P^{•+}); in a subsequent step, P^{•+} oxidizes both Fe³⁺ (to give Fe^{IV}=O) and an amino acid residue. The rate of intramolecular reduction of P^{•+} is 9.8 × 10³ s⁻¹; the rate of ferryl formation is 2.9 × 10³ s⁻¹. Strong EPR signals attributable to tyrosine and tryptophan radicals were recorded after RuC7MbM³⁺ (M = Fe, Mn) was flash-quenched/frozen.

Introduction

Highly oxidized iron–porphyrin intermediates are implicated in the catalytic cycles of many heme enzymes.^{1,2} An example is peroxidase compound **I**, which contains an oxoiron(IV)–radical (ferryl–radical) heme, P^{•+}Fe^{IV}=O (P^{•+} = porphyrin cation radical)³ or R^{•+}Fe^{IV}=O (R = protein-based amino acid).^{4–8} Interestingly, compound **I** is not produced by peroxidation of dioxygen carriers, such as

myoglobin (Mb) and hemoglobin, where P^{•+} is reduced by a protein amino acid residue, giving compound **II** and R[•].^{9–12} Using a Ru–linker–(heme)-modified Mb, Hamachi and co-workers demonstrated that a highly reactive protein–P^{•+}–Fe³⁺ species can be produced photochemically, and that P^{•+}Fe³⁺ undergoes intramolecular electron transfer (ET) (in a pH-dependent step) to give ferryl myoglobin.^{13,14}

Interestingly, Hamachi did not report P^{•+} reduction by R, a reaction that could have been competitive with ferryl formation. In an attempt to elucidate any R → P^{•+} pathways, we prepared a Ru–linker–(heme) similar to the probe employed earlier and inserted it into Mb. We have found that P^{•+} is rapidly reduced (~10⁴ s⁻¹ at pH 7) by one or more amino acid residues in the protein.

* Authors to whom correspondence should be addressed. E-mail: pfarmer@uci.edu (P.J.F.); hbgray@caltech.edu (H.B.G.).

[†] University of California.

[‡] California Institute of Technology.

- (1) Ortiz de Montellano, P. R. *Annu. Rev. Pharmacol. Toxicol.* **1992**, *32*, 89–107.
- (2) Sono, M.; Roach, M. P.; Coulter, E. D.; Dawson, J. H. *Chem. Rev.* **1996**, *96*, 2841–2887.
- (3) Hiner, A. N. P.; Raven, E. L.; Thorneley, R. N. F.; García-Cánovas, F.; Rodríguez-López, J. N. *J. Biol. Inorg. Chem.* **2002**, *7*, 27–34.
- (4) Huyett, J. E.; Doan, P. E.; Gurbel, R.; Houseman, A. L. P.; Sivaraja, M.; Goodin, D. B.; Hoffman, B. M. *J. Am. Chem. Soc.* **1995**, *117*, 9033–9041.
- (5) Stubbe, J.; van der Donk, W. A. *Chem. Rev.* **1998**, *98*, 705–762.
- (6) Pesavento, R. P.; Van Der Donk, W. A. *Adv. Protein Chem.* **2001**, *58*, 317–385.
- (7) Chouchane, S.; Giroto, S.; Yu, S. W.; Magliozzo, R. S. *J. Biol. Chem.* **2002**, *277*, 42633–42638.
- (8) Ivancich, A.; Jakopitsch, C.; Auer, M.; Un, S.; Obinger, C. *J. Am. Chem. Soc.* **2003**, *125*, 14093–14102.

- (9) Gibson, J. F.; Ingram, D. J. E.; Nicholls, P. *Nature* **1958**, *181*, 1398–1399.
- (10) He, B.; Sinclair, R.; Copeland, B. R.; Makino, R.; Powers, L. S.; Yamazaki, I. *Biochemistry* **1996**, *35*, 2413–2420.
- (11) Gunther, M. R.; Tschirret-Guth, R. A.; Lardinois, O. M.; Ortiz de Montellano, P. R. *Chem. Res. Toxicol.* **2003**, *16*, 652–660.
- (12) Svistunenko, D. A.; Dunne, J.; Fryer, M.; Nicholls, P.; Reeder, B. J.; Wilson, M. T.; Bigotti, M. G.; Cutruzzola, F.; Cooper, C. E. *Biophys. J.* **2002**, *83*, 2845–2855.
- (13) Hamachi, I.; Tsukiji, S.; Shinkai, S.; Oishi, S. *J. Am. Chem. Soc.* **1999**, *121*, 5500–5506.
- (14) Hamachi, I.; Takashima, H.; Hu, Y. Z.; Shinkai, S.; Oishi, S. *Chem. Commun.* **2000**, *13*, 1127–1128.

Experimental Section

General Procedures. Absorption spectra were recorded with a Hewlett-Packard 8453 diode array spectrophotometer. Emission spectra were measured with a Hitachi F4500 fluorimeter. The excitation source for transient absorption experiments was a Nd:YAG laser tuned to 480 nm with an OPO (Continuum). Probe light was provided by a 75 W Xe arc lamp, dispersed by a monochromator, and detected with a photomultiplier tube. The photomultiplier tube output was amplified and processed by a Tektronix oscilloscope interfaced to a PC. Kinetics traces were analyzed with a least-squares fitting procedure (MicroCal Origin). Transient absorption measurements were conducted at 22 ± 2 °C using 1 cm quartz cuvettes fitted with vacuum side arms. Samples were degassed with N_2 by repetitive vacuum/fill cycles using a Schlenk line. Solutions for transient absorption measurements (2–3 mL) were typically 4–6 μ M protein/saturated $[Co(NH_3)_5Cl]Cl_2/NaP_i$ buffer (pH 7.0). Fluoride inhibition experiments were carried out in solutions containing 500 mM NaF/saturated $[Co(NH_3)_5Cl]Cl_2/NaP_i$ buffer. Complete conversion to heme–fluoride complex was verified by UV–vis absorption spectroscopy. X-band EPR spectra were recorded with a Bruker EMX spectrometer equipped with a standard TE₁₀₂ (ER 4102ST) or a high-sensitivity (ER 4119HS) resonator (Bruker). A built-in frequency counter provided accurate resonant frequency values. Variable-temperature EPR experiments were performed with an ESR900 continuous-flow helium cryostat (Oxford Instruments).

BpyC7Br. A 1.50 g (0.00817 mol) sample of 4,4'-(CH₃)₂bpy (bpy = 2,2'-bipyridine) in 200 mL of dry THF was cooled to 0 °C under N_2 in a flame-dried flask. A 4.5 mL (0.00902 mol) sample of lithium diisopropylamide was added dropwise and the reaction stirred for 30 min followed by addition of 12.6 mL (0.0820 mol) of 1,6-dibromohexane. The reaction mixture was stirred for 2 h and then dried. The oil was dissolved in $CHCl_3$ and flash-filtered through silica gel (with $CHCl_3$) to remove lithium salts. The product was concentrated and purified by silica gel chromatography. BpyC7Br was eluted as the major fraction with $CHCl_3/(CH_3)_2CO/MeOH$ (17:2:1): yield 1.70 g (85%); ¹H NMR ($CDCl_3$, 500 MHz) δ 8.53 (2H, d, Ar H), 8.21 (2H, s, Ar H), 7.11 (2H, d, Ar H), 3.38 (2H, t, BrCH₂–), 2.68 (2H, t, –CH₂–), 2.42 (3H, s, ArCH₃), 1.82 (2H, m, –CH₂–), 1.68 (2H, m, –CH₂–), 1.35 (6H, m, –CH₂CH₂–CH₂–); FABMS *m/e* 347 (M + 1, 15). Anal. Calcd for C₁₈H₂₃N₂Br: C, 62.25; H, 6.68. Found: C, 62.12; H, 6.92.

BpyC7Ph. To a degassed solution of 0.691 g (0.00187 mol) of bpyC7Br in 10 mL of dry DMF was added 0.417 g (0.00225 mol) of potassium phthalamide. The solution was refluxed for 3 h under N_2 . After the DMF was removed, the solid was dissolved in $CHCl_3$ and purified on a silica gel column, which was eluted with $CHCl_3$: yield 0.675 g (87%); ¹H NMR ($CDCl_3$, 500 MHz) δ 8.51 (2H, d, Ar H), 8.19 (2H, s, Ar H), 7.80 (2H, d, Ar H), 7.67 (2H, d, Ar H), 7.09 (2H, d, Ar H), 3.64 (2H, t, –CH₂Ar), 2.65 (2H, t, –CH₂Ar), 2.41 (3H, s, ArCH₃), 1.66 (6H, m, –CH₂CH₂CH₂–), 1.33 (6H, m, –CH₂CH₂CH₂–); FABMS *m/e* 414 (M + 1, 49). Anal. Calcd for C₂₆H₂₇O₂N₃: C, 74.52; H, 6.68. Found: C, 75.50; H, 6.53.

BpyC7NH₂. A solution of 1.37 g (0.00331 mol) of bpyC7Ph in 12 M HCl (100 mL) was refluxed for 14 h. HCl was removed and the solid dissolved in water (200 mL). The solution was filtered, 0.2 g of KOH added, and then the product extracted with *sec*-butanol (3 × 75 mL) and concentrated. The yellow oil was dissolved in $CHCl_3$ (100 mL), dried over $MgSO_4$, and concentrated to give the amine product: yield 0.79 g (84%); ¹H NMR ($CDCl_3$, 500 MHz) δ 8.52 (2H, d, Ar H), 8.21 (2H, s, Ar H), 7.12 (2H, d, Ar H), 2.67 (2H, t, –CH₂NH₂), 2.64 (2H, t, ArCH₂–), 2.42 (3H,

s, ArCH₃), 1.68 (2H, m, –CH₂–), 1.41 (2H, m, –CH₂–), 1.34 (6H, m, –CH₂CH₂CH₂–); FABMS *m/e* 284 (M + 1, 42).

C7PP. Protoporphyrin IX monomethyl ester (PPME) was prepared according to a literature procedure.¹⁵ A 0.178 g (0.00052 mol) sample of PPME and 0.3 g of bpyC7NH₂ (0.00063 mol) were dissolved in dry THF (100 mL). The solution was transferred to a flame-dried flask and degassed at 0 °C. A 0.15 mL (0.0011 mol) sample of dry triethylamine was added and the solution cooled for 10 min followed by addition of 0.726 mL (0.0011 mol) of diethyl cyanophosphate. The mixture was stirred under N_2 (at room temperature) for 2 days before the solvent was removed. The solid was dissolved in $CHCl_3$, washed with 5% aqueous $NaHCO_3$ (3 × 30 mL), and dried over Na_2SO_4 and the solvent removed. The solid was purified by silica gel chromatography (eluted with 1% $MeOH-CHCl_3$): yield 0.264 g (60%); ¹H NMR ($CDCl_3$, 500 MHz) δ 10.10 (4H, m), 8.42 (2H, d), 8.24 (2H, m), 8.14 (H, s), 7.99 (H, s), 7.00 (H, d), 6.81 (H, d), 6.39 (2H, d), 6.15 (2H, d), 5.98 (H, m), 4.37 (4H, t), 3.68 (3H, s), 3.59 (3H, s), 3.42 (3H, s), 3.24 (2H, t), 3.06 (4H, m), 2.35 (3H, s), 2.11 (2H, t), 0.95 (4H, m), 0.56 (6H, m); FABMS *m/e* 843 (M + 1, 100); UV–vis ($CHCl_3$) λ (nm) 282, 408 (Soret), 542, 576, 631. Anal. Calcd for C₅₃H₅₉N₇O₃: C, 75.59; H, 7.06. Found: C, 74.25, H, 7.4.

RuC7PP. A 0.12 g (0.00014 mol) sample of C7PP and 0.0835 g (0.00017 mol) of $[Ru(bpy)_2Cl_2]$ (Strem) were dissolved in dry, degassed DMF. The solution was refluxed for 24 h (under N_2). The DMF was removed and the solid suspended in H_2O and filtered. The solid was hydrolyzed in basic THF. The solvent was removed and the solid washed with H_2O and dried under vacuum: yield 95%; UV–vis λ_{MeOH} (nm) 287, 403 (Soret), 485, 505, 539, 575.

RuC7MbM³⁺. The Fe³⁺ and Mn³⁺RuC7 complexes were generated by refluxing 0.169 g (0.00014 mol) of RuC7PP and 0.270 g (0.0014 mol) of $FeCl_2$ or 0.242 g of $Mn(OAc)_2$ in dry DMF under N_2 for 6 h. The solvent was removed and the solid washed with 1 M HCl and filtered. The solid was dissolved in $MeOH$ and purified on Sephadex LH-20. Data for RuC7Fe³⁺: yield 80%; ESI MS *m/z* 665 (for methyl ester); UV–vis λ_{MeOH} (nm) 288, 397 (Soret), 592. Data for RuC7Mn³⁺: yield 85%; UV–vis λ_{MeOH} (nm) 287, 371, 463, 547, 582. Apomyoglobin was prepared from equine skeletal muscle myoglobin (Sigma) according to a literature method.¹⁶ A 5-fold excess of RuC7M³⁺ in dimethyl sulfoxide (DMSO) was added dropwise to a solution containing apoprotein at 4 °C such that the final DMSO concentration was less than 10%. The solution was allowed to stir for 12 h at 4 °C before it was dialyzed against 20 mM NaP_i buffer (pH 7) to remove the DMSO. The dialyzed solution was centrifuged and purified by size exclusion chromatography (Sephadex G-25). The protein was concentrated using ultrafiltration units (Centricon YM3 or YM10). Insertion of RuC7M³⁺ into apomyoglobin was followed by UV–vis absorption spectroscopy, $\lambda_{max}(RuC7MbFe^{3+})$ 409 nm.

Results and Discussion

Insertion of RuC7M³⁺ (M = Fe, Mn) into Mb gives RuC7MbM³⁺ (Figure 1). The absorption spectrum of RuC7MbFe³⁺ confirms that the pendant arm does not perturb the native fold nor the region around the heme pocket (Figure 2). The emission of electronically excited RuC7MbFe³⁺ is substantially quenched relative to that of $*[Ru(bpy)_3]^{2+}$: transient absorption measurements demonstrate that quench-

(15) Tsuchida, E.; Nishide, H.; Sato, Y.; Kaneda, M. *Bull. Chem. Soc. Jpn.* **1982**, *55*, 1890–1895.

(16) Martinis, S. A.; Sotiriou, C.; Chang, C. K.; Sligar, S. G. *Biochemistry* **1989**, *28*, 879–884.

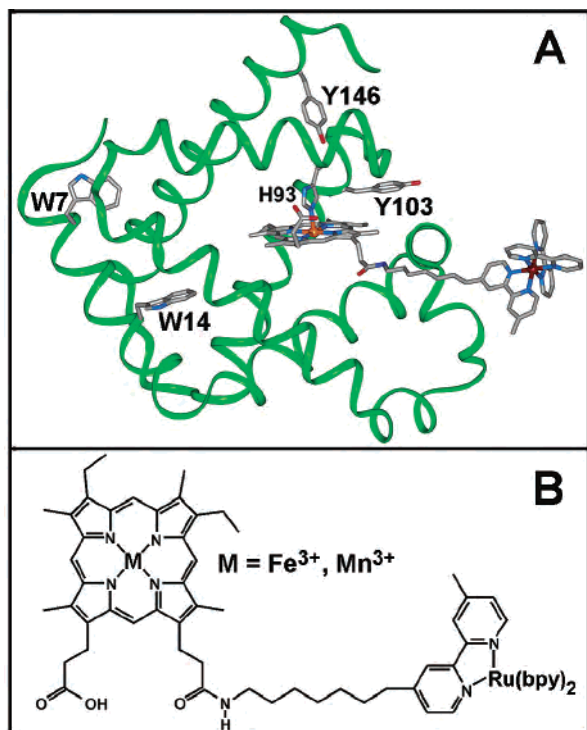


Figure 1. (A) RuC7Mb model based on the horse heart Mb structure³⁶ (PDB code 1YMB). (B) RuC7.

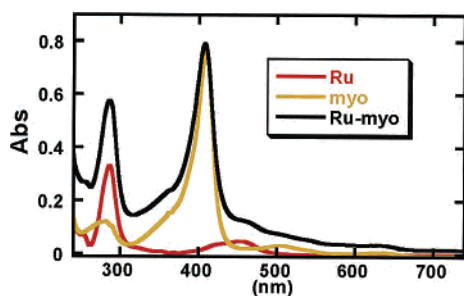


Figure 2. Absorption spectra of (Ru) [Ru(bpy)₃]²⁺, (myo) MbFe³⁺, and (Ru-my) RuC7MbFe³⁺ (~4 μM) in NaP₁ buffer (pH 7).

ing is due in part to $*\text{Ru}^{2+}\text{Fe}^{3+} \rightarrow \text{Ru}^{3+}\text{Fe}^{2+}$ ET ($k > 10^8 \text{ s}^{-1}$); the rate of charge recombination ($\text{Ru}^{3+}\text{Fe}^{2+} \rightarrow \text{Ru}^{2+}\text{Fe}^{3+}$) is $1.4 \times 10^7 \text{ s}^{-1}$ (Figure S1 in the Supporting Information).¹⁷

Irreversible oxidative flash-quenching experiments (Scheme 1)^{18,19} show that $\text{P} \rightarrow \text{Ru}^{3+}$ ET ($-\Delta G^\circ \approx 0.4 \text{ eV}$ vs NHE) to form P^{*+} is very fast (Figure 3). The kinetics of P^{*+} reduction are biphasic (Figures 3A, S2, and S3). Inhibition of ferryl formation (by addition of a large excess of NaF) produced similar absorption changes (Figures 3B and S4); under these conditions, P^{*+} decays exponentially with a rate ($9.8 \times 10^3 \text{ s}^{-1}$, pH 7) that depends on pH but not on protein/quencher concentration.²⁰ We assign $\text{R} \rightarrow \text{P}^{*+}$ ET as the main P^{*+} reduction pathway in RuC7Mb.²¹ Fitting the biphasic P^{*+} reduction kinetics trace with a fixed value (9.8×10^3

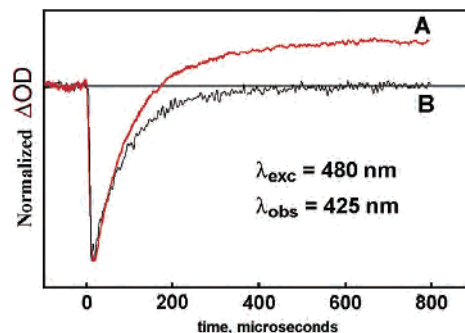
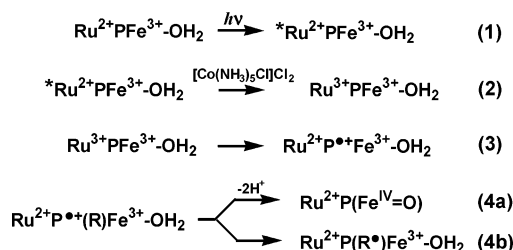


Figure 3. Transient absorption traces monitored at P^{*+} and ferryl Soret ($\lambda_{\text{max}} 425 \text{ nm}$) wavelengths for solutions containing RuC7MbFe³⁺/[Co(NH₃)₅Cl]²⁺ in the absence (A) and presence (B) of 500 mM NaF (see Figure S4). In the absence of F⁻ less than 30% of the P^{*+} is converted to ferryl.

Scheme 1



s^{-1}) for the major component ($\text{R} \rightarrow \text{P}^{*+}$ ET) yielded a rate of $2.9 \times 10^3 \text{ s}^{-1}$ for ferryl formation at pH 7.²²

Horse heart myoglobin contains four aromatic amino acid residues, Y103, Y146, W7, and W14 (Figure 1A), whose reduction potentials should fall in the 0.6–1.0 V vs NHE^{23–25} range and could, therefore, be oxidized by P^{*+} or $\text{Fe}^{\text{IV}}=\text{O}$.^{10,26} We trapped protein-based radical species by photolysis/freeze-quenching of solutions containing RuC7MbM³⁺/[Co(NH₃)₅Cl]²⁺, as evidenced by strong EPR signals centered at $g \approx 2.004$ (Figures 4 and 5).²⁷ An intense EPR signal with $\Delta H_{\text{pp}} = 15 \text{ G}$ (ΔH_{pp} is the peak-to-trough line width) and partially resolved hyperfine structure was observed in experiments conducted on degassed solutions containing RuC7MbFe³⁺/[Co(NH₃)₅Cl]²⁺ (Figure 4A); this spectrum features a composite signal with a substantial contribution from a neutral Y radical,³³ possibly Y103, as this residue is

(20) In model compounds, the $\text{P}^{*+}\text{Fe}^{3+}/\text{PFe}^{3+}$ potential is largely unaffected by axial ligands, such that the driving force for intramolecular ET should be about the same in the fluoride adduct of RuC7MbFe³⁺ (Hickman, D. L.; Nanthakumar, A.; Goff, H. M. *J. Am. Chem. Soc.* **1988**, *110*, 6384–6390).

(21) We have not detected Y/W radicals optically, as Y^* (~410 nm) and W^* (~530 nm) absorptions are totally masked by intense heme Soret and Q bands.

(22) Ferryl formation occurs over 20 μs in RuC7MbFe³⁺ (pH 7), in contrast to 200 μs in microperoxidase-8 (pH 8) and 500 ms in horseradish peroxidase (pH 8.5).^{18,19} The tightly bound water in the distal pocket of *mer*-Mb facilitates ferryl formation in RuC7Mb in comparison to microperoxidase-8, which apparently undergoes rapid H₂O exchange, or horseradish peroxidase, which undergoes very slow H₂O binding.

(23) Harriman, A. *J. Phys. Chem.* **1987**, *91*, 6102–6104.

(24) Tommos, C.; Skalicky, J. J.; Pilloud, D. L.; Wand, A. J.; Dutton, P. L. *Biochemistry* **1999**, *38*, 9495–9507.

(25) Defelippis, M. R.; Murthy, C. P.; Faraggi, M.; Klapper, M. H. *Biochemistry* **1989**, *28*, 4847–4853.

(26) Farhangrazi, Z. S.; Sinclair, R.; Powers, L.; Yamzaki, I. *Biochemistry* **1995**, *34*, 14970.

(27) Di Bilio, A. J.; Crane, B. R.; Wehbi, W. A.; Kiser, C. N.; Abu-Omar, M. M.; Carlos, R. M.; Richards, J. H.; Winkler, J. R.; Gray, H. B. *J. Am. Chem. Soc.* **2001**, *123*, 3181–3182.

(17) Bjerrum, M. J.; Casimiro, D. R.; Chang, I.-J.; Di Bilio, A. J.; Gray, H. B.; Hill, M. G.; Langen, R.; Mines, G. A.; Skov, L. K.; Winkler, J. R.; Wuttke, D. S. *J. Bioenerg. Biomembr.* **1995**, *27*, 295–302.

(18) Berglund, J.; Pascher, T.; Winkler, J. R.; Gray, H. B. *J. Am. Chem. Soc.* **1997**, *119*, 2464–2469.

(19) Low, D. W.; Winkler, J. R.; Gray, H. B. *J. Am. Chem. Soc.* **1996**, *118*, 117–120.

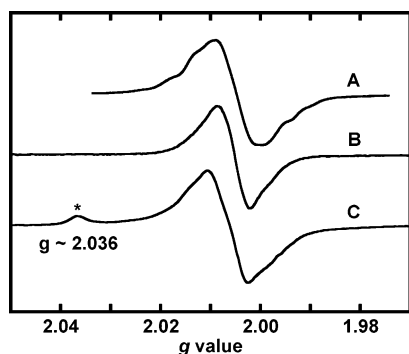


Figure 4. X-band EPR spectra (normalized intensities) of frozen solutions of irradiated samples containing RuC7MbFe³⁺ and saturated (~12 mM) [Co(NH₃)₅Cl]Cl₂ in 25 mM KP_i buffer: samples, held in quartz EPR tubes (4 mm OD) with vacuum side arms, were illuminated while being cooled in an unsilvered Dewar filled with liquid nitrogen. Under these conditions, the time required for thermal equilibration is on the order of 1 s. Photolysis occurred in fluid rather than frozen solution, as no EPR signals were observed from irradiated frozen samples.²⁷ Samples were degassed at room temperature by pump/fill cycles using a Schlenk line prior to photolysis/freeze-quenching. The excitation source was a focused beam from a 300 W Xe lamp (model PE300BF, Perkin-Elmer); suitable filters were used to remove UV light. (A) Degassed RuC7MbFe³⁺ (77 K, $\nu = 9.478$ GHz, microwave power 2 mW, modulation amplitude 3 G). (B) EPR spectrum of sample A after thawing and refreezing without further irradiation (77 K, $\nu = 9.3952$ GHz). (C) Undegassed sample of RuC7MbFe³⁺ (77 K, $\nu = 9.3935$ GHz). $g \approx 2.036$ (marked with an asterisk) is indicative of peroxo species.

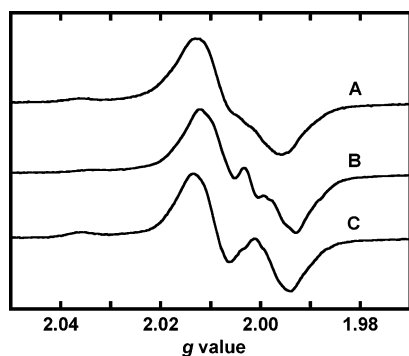


Figure 5. X-band EPR spectra (normalized intensities) of frozen solutions of irradiated samples containing RuC7MbMn³⁺ and saturated (~12 mM) [Co(NH₃)₅Cl]Cl₂ in 25 mM KP_i buffer (see the Figure 4 caption). (A) Degassed RuC7MbMn³⁺ (77 K). (B) Degassed RuC7MbMn³⁺ in D₂O/KP_i (80 K, $\nu = 9.4700$ GHz, microwave power 1 mW, modulation amplitude 1 G). (C) RuC7MbMn³⁺ in the presence of air (77 K).

very close to the heme.^{11,12,28,29} Formation of a peroxo radical (identified by its rhombic \mathbf{g} tensor, $g_z = 2.036$, $g_x = 2.009$, $g_y = 2.003$)³⁰ when photolysis was conducted in air (Figure 4C) demonstrates unambiguously that W14 also is oxidized.^{11,31} Upon thawing and refreezing (a process that took >40 s), a narrower ($\Delta H_{pp} = 8.8$ G) EPR signal having ~20% of the intensity of the initial signal in Figure 4A with no sign of a peroxo species was observed (Figure 4B).³² This

EPR spectrum is significantly sharper (indicating less hyperfine coupling)³³ than those of well-characterized Y[•] and W[•] radicals, which typically have $\Delta H_{pp} > 18$ G,^{5,6} and remains unassigned.³⁴ Importantly, a different radical ($\Delta H_{pp} \approx 31$ G) formed in photolysis experiments conducted on RuC7MbMn³⁺ (Figure 5). On the basis of its hyperfine pattern and spectral width, we assign the signal in Figure 5B (obtained in D₂O/KP_i solution) to W14[•].³⁵ Thus, W14 is oxidized in all our flash-quenching RuC7MbM³⁺ experiments, thereby accounting for the observation that W14–O₂[•] is a final product. However, Y[•] is the prevalent radical species formed at pH 7 in RuC7MbFe³⁺ (ferryl ($E^\circ \approx 0.9$ V vs NHE)¹⁰ is not required for the generation of Y[•] as an EPR signal very similar to that shown in Figure 4A is observed in experiments conducted on protein samples containing excess F⁻).^{10,28} The observation that W[•] is formed preferentially in RuC7MbMn³⁺ suggests that the reduction potential of P⁺ is less positive in Mn³⁺ myoglobin. At pH 7, tyrosine ($pK_a \approx 14$) is expected to have a higher reduction potential than tryptophan.²⁴ We emphasize, however, that we cannot identify with certainty the initial product(s) of oxidation by P⁺ (or ferryl), owing to the relative long time required for freeze-quenching.

The short lifetime of P⁺ in myoglobin is in sharp contrast to much longer-lived forms in horseradish peroxidase and microperoxidase-8,^{18,19} thereby indicating that the fate of this intermediate is dramatically affected by the protein environment. Apparently protein-to-P⁺ ET protects heme-containing dioxygen carriers, as rapid P⁺ reduction would prevent the formation of high-valent species that would lead to unwanted oxygenase or peroxidase chemistry *in vivo*.

Acknowledgment. We thank Kevin Heinrich, David Khandabi, and Greg Quishair for assistance with the synthesis of RuC7. C.E.I. thanks the UC TSR & TP for a graduate fellowship. M.S.C. thanks the Arnold and Mabel Beckman Undergraduate Scholarship Fund for support. This work was supported by the NSF (P.J.F., Grant CHE-0100774), UROP funding from UCI, and the NIH (H.B.G., Grant DK19038).

Supporting Information Available: Kinetics trace for photo-induced ET experiments on RuC7MbFe³⁺ (Figure S1), flash-quenching kinetics traces for RuC7MbFe³⁺/[Co(NH₃)₅Cl]²⁺ as a function of pH (Figures S2 and S3) and in the presence of NaF (Figure S4), and EPR spectra (Figure S5) (PDF). This material is available free of charge via the Internet at <http://pubs.acs.org>.

IC049741H

(28) Tew, D.; Ortiz de Montellano, P. R. *J. Biol. Chem.* **1988**, *263*, 17880–17886.
 (29) Harris, M. N.; Burchiel, S. W.; Winyard, P. G.; Engen, J. R.; Mobarak, C. D.; Timmins, G. S. *Chem. Res. Toxicol.* **2002**, *15*, 1589–1594.
 (30) Sahlin, M.; Cho, K. B.; Pötsch, S.; Lytton, S. D.; Huque, Y.; Gunther, M. R.; Sjöberg, B. M.; Mason, R. P.; Gräslund, A. *J. Biol. Inorg. Chem.* **2002**, *7*, 74–82.
 (31) DeGray, J. A.; Gunther, M. R.; Tschirret-Guth, R.; Ortiz de Montellano, P. R.; Mason, R. P. *J. Biol. Chem.* **1997**, *272*, 2359–2362. EPR investigations of Mason, Ortiz de Montellano, and their co-workers show that W14 is the only stable peroxidation site in myoglobin and that tyrosine is not required for W14–O₂[•] formation.

(32) The decay of the peroxo radical within 40 s is in accord with the ~7 s lifetime of peroxo radicals in Mb.³⁰ All the radicals observed in photolysis experiments on RuC7Mb, with the exception of the species corresponding to the EPR spectrum in Figure 4B (which persists longer than 2 min), decay within 40 s.
 (33) Kelman, D. J.; Degray, J. A.; Mason, R. P. *J. Biol. Chem.* **1994**, *269*, 7458–7463.
 (34) Subtraction of the EPR signal in Figure 4B from the signal in Figure 4A (taking into account that upon thawing/refreezing the intensity of the first signal is reduced to about 20%) gives a spectrum with a hyperfine pattern that is attributable to a tyrosyl radical (see Figure S5). However, this procedure gives only qualitative results as the actual intensity of the narrow signal prior to thawing/refreezing and the contribution of W14[•] are unknown.
 (35) Miller, J. E.; Gradinaru, C.; Crane, B. R.; Di Bilio, A. J.; Wehbi, W. A.; Un, S.; Winkler, J. R.; Gray, H. B. *J. Am. Chem. Soc.* **2003**, *125*, 14220–14221.
 (36) Evans, S. V.; Brayer, G. D. *J. Mol. Biol.* **1990**, *213*, 885–897.